



The influence of spheroid formation of human adipose-derived stem cells on chitosan films on stemness and differentiation capabilities

Nai-Chen Cheng^{a,b,c}, Shan Wang^b, Tai-Horng Young^{a,c,*}

^aInstitute of Biomedical Engineering, College of Medicine and College of Engineering, National Taiwan University, 1 Jen-Ai Rd., Taipei 100, Taiwan

^bDepartment of Surgery, National Taiwan University Hospital and College of Medicine, Taipei, Taiwan

^cResearch Center for Developmental Biology and Regenerative Medicine, National Taiwan University, Taipei, Taiwan

ARTICLE INFO

Article history:

Received 11 October 2011

Accepted 20 November 2011

Available online 9 December 2011

Keywords:

Spheroid

Adipose-derived stem cell

Chitosan

Stemness

Differentiation

ABSTRACT

Adipose-derived stem cells (ASCs) have valuable applications in regenerative medicine, but maintaining the stemness of ASCs during *in vitro* culture is still a challenging issue. In this study, human ASCs spontaneously formed three-dimensional spheroids on chitosan films. Most ASCs within the spheroid were viable, and the cells produced more extracellular molecules, like laminin and fibronectin. Comparing to monolayer culture, ASC spheroids also exhibited enhanced cell survival in serum deprivation condition. Although cell proliferation was inhibited in spheroids, ASCs readily migrated out and proliferated upon transferring spheroids to another adherent growth surface. Moreover, spheroid-derived ASCs exhibited higher expansion efficiency and colony-forming activity. Importantly, we demonstrated that spheroid formation of human ASCs on chitosan films induced significant upregulation of pluripotency marker genes (*Sox-2*, *Oct-4* and *Nanog*). By culturing the ASC spheroids in proper induction media, we found that ASC differentiation capabilities were significantly enhanced after spheroid formation, including increased transdifferentiation efficiency into neuron and hepatocyte-like cells. In a nude mice model, we further showed a significantly higher cellular retention ratio of ASC spheroids after intramuscular injection of spheroids and dissociated ASCs. These results suggested that ASCs cultured as spheroids on chitosan films can increase their therapeutic potentials.

© 2011 Elsevier Ltd. All rights reserved.

1. Introduction

Mesenchymal stem cells (MSCs), which are capable of self-renewal and multi-lineage differentiation, have been a focus in regenerative medicine research. Unlike embryonic stem cells (ESCs), MSCs do not exhibit pluripotent plasticity, but they represent a potential autologous cell source, which circumvents the complications associated with allogeneic transplantations. Moreover, clinical application of MSCs exhibits virtually no ethical or political issue that encountered with the use of ESCs. Adipose-derived stem cell (ASC) represents an abundant source of MSCs that are easily accessible from subcutaneous adipose tissue via liposuction [1,2]. As many as 1% of adipose cells are estimated to be stem cells, compared to the 0.001–0.002% found in bone marrow, currently a common source of MSCs [3]. In addition to the ability of self-renewal, ASCs can differentiate into multiple lineages when

cultivated under lineage-specific conditions, including osteogenic, adipogenic, and chondrogenic lineages [4]. Recently, ASCs are found to be capable of transdifferentiating into mature cells not related with their original lineage, such as hepatocyte of endoderm origin and neuron of ectoderm origin [5,6]. This ability, together with their easy accessibility and low donor site morbidity, has made ASCs good candidates for a broad range of cell-based therapeutics. The presence of pluripotency markers, including *Oct-4*, *Sox-2* and *Nanog*, is important for the renewal and differentiation capabilities of ASCs [7,8], but they are detected only in cells from early passages [9]. Therefore, maintaining the expression of stemness markers has become an important issue for *in vitro* culture of ASCs.

MSCs are commonly cultured as monolayers using conventional tissue culture techniques. These methods have proved adequate, but several reports have demonstrated a loss of the replicative ability, colony-forming efficiency, and differentiation capacity with time in culture [8,9]. The cellular microenvironment is known to have a profound influence on the biology of the stem cells within it. For example, the differentiation of stem cells is highly regulated by their niche through both intrinsic and extrinsic signals [10]. Hence, the application of three-dimensional (3D) cell culture techniques in stem cell research has received increased interest. The 3D methods

* Corresponding author. Institute of Biomedical Engineering, College of Medicine and College of Engineering, National Taiwan University, 1 Jen-Ai Rd., Taipei 100, Taiwan. Tel.: +886 2 23123456x81455; fax: +886 2 23940049.

E-mail address: thyoung@ntu.edu.tw (T.-H. Young).

facilitate greater cell–cell contacts and interactions of cells with the extracellular matrix (ECM). By allowing cells to adapt to their native morphology, significant differences between the cellular phenotype and biological response of cells cultured in monolayer and 3D environment have been observed [11–13]. Consequently, it is becoming increasingly accepted that 3D culture methods provide a cellular environment more consistent with that *in vivo* [12].

Approaches providing a 3D culture environment included the use of porous scaffolds, hydrogels, and cellular aggregates, each of which have been successfully employed with a variety of cell type [12,14,15]. Among these techniques, cellular aggregates, including cell spheroid and cell sheet, have drawn increasing attention because they are free of exogenous biomaterials that may cause untoward responses upon cell transplantation [16–19]. Moreover, recently there has been a series of publication on aggregation of bone marrow-derived MSCs as a procedure to enhance their therapeutic potential [12,17,20,21]. Although the use of 3D spheroid culture methods holds promise in the field of stem cell research, a large quantity of cells is required for cell spheroid formation and further therapeutic applications [20]. As a result, ASC represents an ideal cell source for spheroid culture because abundant autologous cells can be easily obtained.

Several procedures have been used to induce cellular spheroid formation, including nonadherent culture conditions, high degree of confluency, nutrient deprivation, air–liquid interface, spinner flask and hanging drops [12,20]. Chitosan is a positively charged natural polysaccharide with good biocompatibility [22], and differences in the cell adhesion and proliferation have been found according to the cell type and the degree of deacetylation on chitosan [23–26]. We previously observed spheroid formation of melanocytes and keratocytes on chitosan films, and their cellular phenotypes were maintained in the 3D culture system [23,27]. In this study, we tested whether ASCs also could aggregate to form spheroids on chitosan films and analyzed the influence of spheroid formation on stemness and differentiation capabilities of ASCs. The information should be useful for the development of biomaterials to regulate the proliferation and differentiation of ASCs and their eventual manipulation to replace lost or dysfunctional tissues following trauma or disease.

2. Materials and methods

2.1. Preparation of chitosan-coated culture plates

Chitosan was coated on tissue culture plates using methods described in a previous study, with some modifications [23]. Briefly, 0.5 mL 1% (w/w) chitosan solution (C-3646, Sigma, St. Louis, MO) dissolved in 0.67% (w/v) acetic acid was added into each well of 24-well tissue culture plates (TCPS; Greiner bio-one, Frickenhausen, Germany) and dried in an oven at 60 °C for 24 h to form a thin film, after which it was neutralized by 0.5 N NaOH aqueous solution (Sigma) for 2 h. Next, the plates were washed thoroughly with distilled water before being exposed to ultraviolet light overnight.

2.2. Cell culture

Subcutaneous adipose tissue from abdomen was obtained from patients undergoing elective abdominoplasty procedures. The study protocol was approved by the Internal Ethical Committee of National Taiwan University Hospital. The adipose tissue was placed in a physiological solution (0.9% NaCl), washed twice with phosphate-buffered saline (PBS) and finely minced. The scraped adipose tissue was then placed in a digestion solution: 1 mg/mL collagenase type I (Gibco, Carlsbad, CA) supplemented with 1% penicillin–streptomycin (Biological industries, Kibbutz Beit Haemek, Israel) at 37 °C in agitation for 60 min. The digest was filtered through 70 µm filters (Becton & Dickinson, Sunnyvale, CA). The cell suspension was centrifuged, and the cells were cultured in expansion medium consisting of Dulbecco's modified Eagle's medium (DMEM)/F-12 (Thermo Scientific, Waltham, MA), 10% fetal bovine serum (FBS; Biological industries), 1% penicillin–streptomycin, and 1 ng/mL basic fibroblast growth factor (bFGF; R&D systems, Minneapolis, MN). The cells were cultured at 37 °C in 5% CO₂, and the medium was changed every 2 days. When the cells have reached 90% confluence, the cells were lifted with 0.05% trypsin-EDTA (Biological industries) and replated.

The ASCs were passaged 3 times, at which point they were trypsinized and counted with a hemocytometer. The cell suspension was plated onto chitosan films or TCPS with the culture medium consisting of DMEM-high glucose (DMEM-HG, Gibco), 10% FBS and 1% penicillin–streptomycin. Culture medium was refreshed every 2–3 days. In some experiments, after spheroids were formed on chitosan films 7 days after cell seeding, these spheroids were transferred from chitosan films to a TCPS or a new chitosan film and then cultured for 7 more days. The morphology of the cells was observed under an inverse phase contrast microscope at the indicated times. To determine the appropriate seeding densities that would yield ASC spheroids, ASCs were seeded with the densities of 1.50×10^3 , 3.13×10^3 , 6.25×10^3 , 1.25×10^4 , 2.50×10^4 , and 5.00×10^4 cells/cm² onto chitosan films. To calculate the number and size distribution of spheroids, the entire culture well was photographed by arrays of micrographs under an inverse phase contrast microscope (TS-100, Nikon, Tokyo, Japan). The images were reassembled together, and the number and diameters of spheroids were calculated using the software Image J (<http://rsbweb.nih.gov/ij/>). Only those with the diameter of more than 50 µm were considered spheroids.

For the electron microscopic study, briefly, samples were washed with PBS twice and fixed with 2.5% glutaraldehyde in PBS for 1 h. After thoroughly washing with PBS, the cells were dehydrated by gradual change of concentrated ethanol and then dried by lyophilization. The specimens were then sputter coated with platinum and examined using a scanning electron microscope (JSM-6700F, JOEL, Tokyo, Japan).

2.3. Cell proliferation and viability assay

The alamar blue assay was modified from a previous study for cell proliferation estimation [28]. Day 0 was defined as the day when cells were trypsinized from the flasks and seeded onto the chitosan films or TCPS, and an initial 4 h period was allowed for cell attachment. On days 0, 1, 3, 5, alamar blue solution (AbD Serotec, Kidlington, UK) was directly added into the culture wells, and the plate was further incubated at 37 °C for 24 h. The absorbance of experimental and control wells was read at 570 and 600 nm with a standard spectrophotometer (Tecan, Taipei, Taiwan). The number of viable cells correlated with the magnitude of dye reduction and was expressed as percentage of alamar blue reduction. Three experimental results were shown as an activity index, defined as the normalized ratio of absorbance value to day 0. Moreover, some spheroids were harvested after 7 days of culture and transferred to a TCPS or a new chitosan film. The day that the spheroids were reseeded was defined as day 0, and the alamar blue assay was performed on days 0, 1, 3, 5 and 7. Proliferation of monolayer and spheroid-derived ASCs was also estimated by alamar blue assay on days 0, 1, 3, 6, 9, 12 and 14.

Cell viability was assessed by the trypan blue dye exclusion assay and the calcein AM analysis. At day 1, 3, 5, and 7 of culture on chitosan films or TCPS, ASCs were trypsinized and dissociated. The numbers of viable and dead cells were examined by standard trypan blue dye exclusion assay [23]. Cell viability was calculated as the number of viable cells divided by the total number of cells. Moreover, Live/Dead kit (Invitrogen, Carlsbad, CA) was used to visualize the viable and dead cells in ASC spheroids according to the manufacturer's protocol. The viability of spheroid cells was determined by staining with calcein AM to label the live cells and with ethidium homodimer to label the dead cells. Spheroids were incubated in PBS containing calcein AM and ethidium homodimer at 37 °C for 1 h. After washing twice with PBS, the cells were observed using a confocal microscope (Zeiss LSM 510).

2.4. Flow cytometry

Monolayer and spheroid ASCs were harvested by trypsinization and pipetting to produce a single-cell suspension in an identical manner. To determine cell surface antigen expression, the samples were incubated with the following antibodies: human monoclonal antibodies against PECAM (BD pharmingen, San Jose, CA), CD29 (BD pharmingen), CD34 (BD pharmingen), CD44 (BD pharmingen), CD90 (BD pharmingen), CD105 (eBioscience, San Diego, CA) and CD166 (BD pharmingen). The samples were analyzed using a flow cytometer (FACScan; Becton Dickinson, Franklin Lakes, NJ) which counts 10,000 cells per sample. Positive cells were determined as the proportion of the population with higher fluorescence than 95% of the isotype control.

For apoptosis assays, ASC spheroids and monolayer ASCs were cultured in serum-free medium for 7 days before trypsin dissociation. Spheroids and monolayer ASCs were stained with annexin V-FITC apoptosis detection kit (Strongbiotech, Taipei, Taiwan) according to the supplier's instructions. Cells were analyzed on a FACScan and gated according to forward scatter, side scatter, and their ability to exclude propidium iodide (PI). Annexin V-positive and PI-negative cells were considered apoptotic cells, while annexin V-positive and PI-positive cells were necrotic cells.

2.5. Colony-forming unit-fibroblast (CFU-F) assays

CFU-F assay was performed using modified techniques described previously [29]. Monolayer or spheroid-derived ASCs were cultured in culture medium at a density of 1000 cells per 100 mm dish. The media were changed every 3 days. After 14 days of culture, the cells were fixed with 4% paraformaldehyde and stained with 0.1% crystal violet solution (Sigma). The number of colonies (diameter ≥ 2 mm) was counted.

2.6. Differentiation of human ASCs

For ASCs in monolayer and spheroid culture, adipogenic differentiation was induced in DMEM-F12 supplemented with 10% FBS, 1% penicillin–streptomycin, 500 μM 3-isobutyl-1-methylxanthine (IBMX; Sigma), 1 μM dexamethasone (Sigma), 10 μM insulin (Sigma) and 200 μM indomethacin (Sigma). At day 7, the expression of adipogenic representative gene, *PPAR- γ* , was analyzed. After 2 weeks, monolayer and spheroid cells were fixed in 4% paraformaldehyde and stained with Oil Red O (Sigma) to observe lipid droplets. Osteogenic differentiation was induced by culturing ASC populations in DMEM-HG supplemented with 10% FBS, 1% penicillin–streptomycin, 10 nM dexamethasone, 50 μM ascorbic acid 2-phosphate (Sigma), and 10 mM β -glycerophosphate (Sigma). At day 7, the expression of osteogenic representative gene, *Runx2*, was analyzed. After 2 weeks, monolayer and spheroid ASCs were fixed in 4% paraformaldehyde and stained with Alizarin red S (Sigma) to observe mineralized matrix apposition.

Neurogenic and hepatogenic differentiation of monolayer and spheroid ASCs were selected to test the representative transdifferentiation capacities of ectoderm and endoderm lineages. To induce neurogenic differentiation, the cells were grown in DMEM-HG containing 1% FBS, 1% penicillin–streptomycin, and 100 ng/mL bFGF (R&D) for 7 days, followed by supplementing 10 μM forskolin (Sigma) for another 7 days [30]. Then the expression of neurogenic marker, *Nestin*, was analyzed by reverse transcription-polymerase chain reaction (RT-PCR) and immunofluorescence. For hepatic differentiation, monolayer and spheroid ASCs were cultured in serum-free medium with 20 ng/mL epidermal growth factor (EGF, R&D) and 10 ng/mL bFGF for 48 h. In the following 4 weeks, 4.9 mM nicotinamide (Sigma) was also supplemented in the culture medium [31]. After 30 days of culture, the expression of hepatogenic marker, *Albumin*, was analyzed by RT-PCR and immunofluorescence.

2.7. Real-time quantitative polymerase chain reaction (qPCR)

Total RNAs of ASC spheroids and adhered cells were extracted with TRIzol[®] reagent (Invitrogen) according to manufacturer's instructions. Total RNA concentration was determined by optical density at 260 nm (OD_{260}) using a spectrophotometer (Nanodrop ND-1000; Thermo Scientific). Once RNA was isolated, complementary DNA (cDNA) was synthesized from RNA using High-Capacity cDNA Reverse Transcription Kits (Applied Biosystems, Foster City, CA). The sequences of the gene-specific primers are shown in Table 1. Briefly, qPCR was performed in triplicate using a StepOne[™] Real-Time PCR system (Applied Biosystems). The expression level was analyzed and normalized to β -actin for each cDNA sample. Relative quantity (RQ) of gene expression was calculated with day 0 ASC samples obtained before cell seeding as the reference point.

2.8. Western blot

The protein expression of *Sox-2*, *Oct-4* and *Nanog* transcription factors was determined at day 7 of cell culture. Monolayer cells and ASC spheroids were resuspended in cell lysis buffer (Thermo scientific) and sonicated. After centrifugation, the protein content was determined in the supernatants by a BCA protein quantification kit (Pierce Biotechnology, Rockford, IL). Sixty μg proteins from spheroids or monolayer cells were added to Laemmli sample buffer and boiled for 10 min. Proteins were separated by sodium dodecyl sulfate-polyacrylamide gel electrophoresis (SDS-PAGE) and blotted onto polyvinylidene difluoride membranes. Western blot was performed using anti-*Oct-4* (Genetex, Irvine, CA), anti-*Sox-2* (R&D systems), anti-*Nanog* (R&D systems), and anti- β -actin (Millipore, Billerica, MA). The

membranes were incubated with the primary antibodies overnight at 4 °C. After extensive washing, the membranes were further incubated with horseradish peroxidase-conjugated secondary antibodies for 1 h. The blots were then developed using an enhanced chemiluminescence detection system (Millipore).

2.9. Immunofluorescence and immunohistochemistry

The retrieved samples were fixed in 4% phosphate-buffered paraformaldehyde, embedded in paraffin, and sectioned into a thickness of 5 μm . For immunofluorescence staining, specimens were de-waxed, rehydrated through a graded series of ethanol, washed twice with PBS, and immersed in 0.1% Triton X-100 for 10 min at room temperature, followed by washing 3 times with PBS. The following primary antibodies were incubated overnight at 4 °C: anti-*Oct-4* (Genetex), anti-*Nanog* (R&D systems), anti-*Sox-2* (R&D systems), anti-SSEA-4 (R&D systems), anti-*Nestin* (Abcam, Cambridge, MA), and anti-Human Serum Albumin (Abcam). After incubation with primary antibodies, cells were washed with PBS and then incubated with fluorescence-conjugated secondary anti-Goat IgG (Genetex) or anti-mouse IgG (Santa Cruz, Santa Cruz, CA) for 1 h at room temperature. After nuclear staining with 4',6-diamidino-2-phenylindole (DAPI, Santa Cruz), slides were mounted and analyzed with a fluorescent microscope (Leica DMI 6000).

Immunohistochemical analysis was performed using antibodies for anti-fibronectin (Epitomics, Burlingame, CA) and anti-laminin (Thermo Scientific). Bovine serum albumin (BSA, Santa Cruz) was used on all sections before secondary antibody labeling, followed by subsequent linking to horseradish peroxidase and substrate/chromogen reaction using immunoperoxidase secondary detection kit (Millipore). Negative controls without utilizing primary antibodies were also prepared to rule out nonspecific labeling.

2.10. Animal study

The animal study was approved by the Animal Care and Use Committee of National Taiwan University, Taipei, Taiwan. Female nude mice (20–25 g body weight; National Laboratory Animal Center, Taipei, Taiwan) were used in this study. The mice were anesthetized with xylazine (5 mg/kg) and methyl-4-hydroxybenzoate (0.3 mg/kg). ASC spheroids and monolayer ASCs with identical cell numbers (1×10^6 cells) were suspended in PBS respectively and transplanted into the skeletal muscle of mice hindlimbs using 27-gauge needles. Each studied animal received two injections: ASC spheroids transplantation for the left hindlimb, and monolayer ASCs for the right hindlimb. The transplanted cells along with the surrounding tissues were retrieved 1 or 3 weeks postoperatively ($n = 4$ at each time point). Immunohistochemical analysis was performed using anti-human nuclear antigen (HNA, Chemicon) to identify the transplanted cells in the skeletal muscle. The stained sections were examined and photographed under microscope. The transplanted ASCs were identified by positive immunostaining and counted. The number of human ASC per high power field was calculated after examining 10 randomly selected fields per sample.

2.11. Statistical analysis

All measurements are presented as mean \pm standard deviation (SD). Statistical significance was evaluated using independent-samples Student's *t*-test or ANOVA followed by Scheffé's post-hoc test. The analyses were performed using STATA software (Stata Inc, College Station, TX). Statistically significant values were defined as $p < 0.05$.

3. Results

3.1. Formation of ASC spheroids

Only suspended ASCs or the spheroids were observed on the chitosan films with very few adhered cell. On day 1, ASCs on chitosan films started forming spheroids in the groups with higher seeding densities. On day 3, cells began to form various sizes of spheroids, and the number of suspended cells decreased markedly. The size of spheroids increased gradually on day 5 and day 7, while the number of suspended cells continued to decrease (Fig. 1). On day 7, when the initial cell densities were 1.50×10^3 , 3.13×10^3 , 6.25×10^3 , 1.25×10^4 , 2.50×10^4 , and 5.00×10^4 cells/cm², the average number of spheroids in 2 cm² of cultured area was 13.5 ± 2.9 , 26.3 ± 10.4 , 33.0 ± 4.2 , 28.5 ± 8.7 , 54.0 ± 11.2 , and 47.0 ± 6.9 , respectively; the average spheroid diameter was 76.7 ± 41.2 , 85.9 ± 43.0 , 106.1 ± 43.8 , 136.0 ± 69.5 , 144.5 ± 55.1 and 194.6 ± 43.3 μm , respectively. The dynamic processes of ASC spheroid formation on chitosan membranes were recorded by the

Table 1
Primer sequences used for the real-time RT-PCR analysis.

Target gene		Primer sequences
<i>β-actin</i>	Forward	5'-CATGTACGTTGCTATCCAGGC-3'
	Reverse	5'-CTCCTTAATGTACGCACGAT-3'
<i>Oct-4</i>	Forward	5'-GCAGCGACTATGCACAACGA-3'
	Reverse	5'-CCAGAGTGGTGACGGAGACA-3'
<i>Sox-2</i>	Forward	5'-CATCACCCACAGCAAATGACA-3'
	Reverse	5'-GCTCTACCGTACCCTAGAACTT-3'
<i>Nanog</i>	Forward	5'-CCTGTGATTGTGGGCTG-3'
	Reverse	5'-GACAGTCTCCGTGTGAGGCAT-3'
<i>Runx2</i>	Forward	5'-TTCATCCCTCACTGAGAG-3'
	Reverse	5'-TCAGCGTCAACACCATCA-3'
<i>PPAR-γ</i>	Forward	5'-TCAGGTTTGGGCGGATGC-3'
	Reverse	5'-TCAGCGGGAAGGACTTTATGTATG-3'
<i>MAP2</i>	Forward	5'-CCAATGGATCCCATACAGG-3'
	Reverse	5'-CTGCTACAGCCTCAGCAGTG-3'
<i>Nestin</i>	Forward	5'-GGCAGCGTTGGAACAGAGGT-3'
	Reverse	5'-CATCTTGAGGTGCGCCAGCT-3'
<i>Albumin</i>	Forward	5'-TGTTCATGAGAAAACGCCA-3'
	Reverse	5'-GTCGCCTGTTCCACCAAGGA-3'

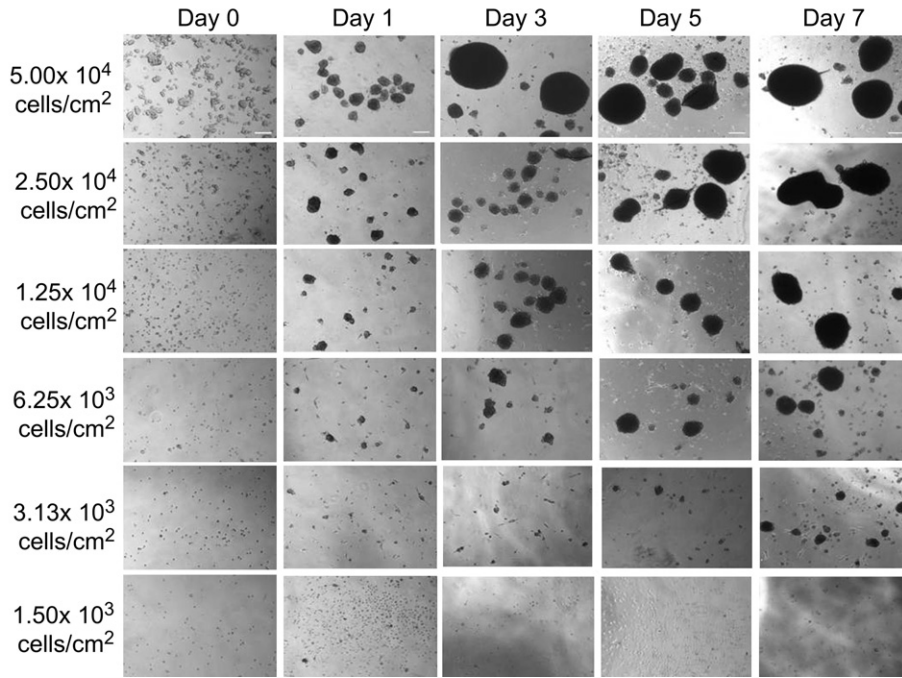


Fig. 1. The relationship between seeding densities and the formation of ASC spheroids. Human ASCs were seeded onto chitosan films in the densities of 1.50×10^3 , 3.13×10^3 , 6.25×10^3 , 1.25×10^4 , 2.50×10^4 , and 5.00×10^4 cells/cm². Scale bars: 150 μ m.

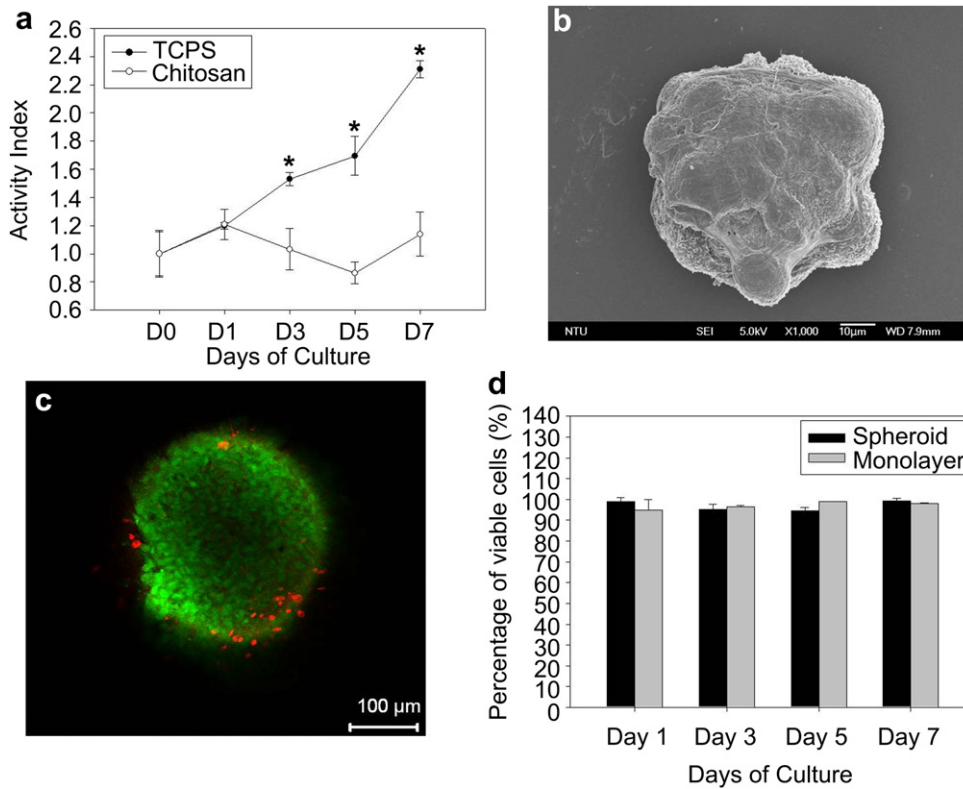


Fig. 2. (a) Alamar blue assays of ASCs cultured on TCPS (solid circle) and chitosan films (empty circle) at the initial seeding density of 2.50×10^4 cells/cm². The activity index was defined as a ratio of absorbance value of formazan relative to that of day 0, which was the seeding day. (b) Scanning electron microscopic image of ASC spheroids after 7 days of culture revealed an indistinguishable cell–cell junction. Scale bar: 10 μ m. (c) Confocal microscopic image of Live/Dead stain on day 7. The section was 50 μ m from the spheroid surface. Live cells were stained by calcein AM (green), and dead ones were stained with ethidium homodimer (red). Scale bar: 100 μ m. (d) The ratio of live and dead cells in the spheroid was determined by trypan blue exclusion assay on day 1, 3, 5, and 7. No significant difference between the spheroid and monolayer culture was noted on either day ($n = 3$). (For interpretation of the references to colour in this figure legend, the reader is referred to the web version of this article.)

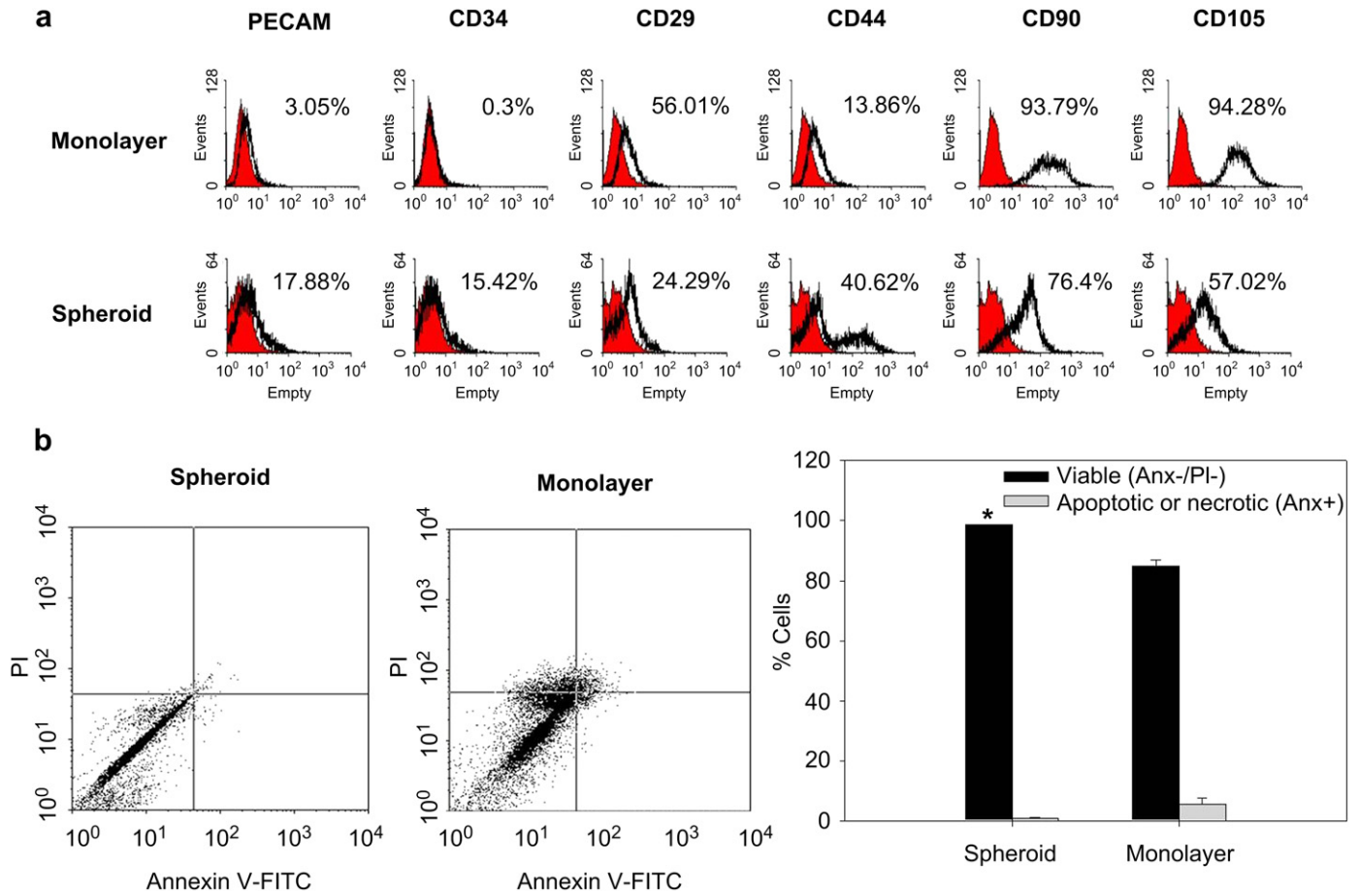


Fig. 3. Phenotypic characterization of ASCs derived from spheroid and monolayer cultures. (a) The expression level of ASC surface antigens was determined after 7 days of monolayer and spheroid cultures. Percentages shown are the proportion of positively stained cells relative to an isotype control. (b) Viability of ASCs under serum-free culture condition was determined by flow cytometry measuring PI uptake and annexin V-FITC labeling. Representative log fluorescent dot plots and summary of the data are shown. The percentage of viable cells was significant higher in the group of spheroid culture. * $p < 0.05$, compared to the monolayer group ($n = 3$).

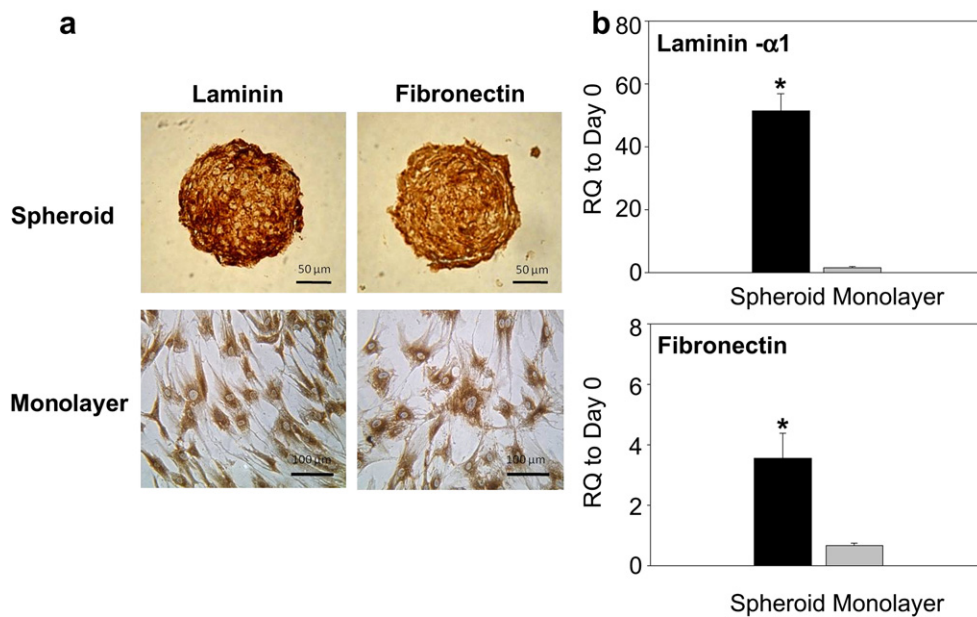


Fig. 4. (a) Immunohistochemical images of fibronectin and laminin in ASC spheroid and monolayer after 7 days of culture. Scale bar: spheroid, 50 μm ; monolayer, 100 μm . (b) RT-PCR analysis showed significantly upregulated *Fibronectin* and *Laminin- $\alpha 1$* genes in spheroid culture. Data presented as mean relative quantity (RQ) \pm SD; * $p < 0.05$, compared to the monolayer group ($n = 3$).

Cultured Cell Monitoring System and typical time-lapse images are included in the [supplementary video file](#). On chitosan films, ASCs were very motile and spontaneously aggregated into multicellular spheroid after intercellular collision. These small aggregates were also highly motile, and they merged with each other as well as isolated cells to form a bigger spheroid.

Dense cellular structures develop hypoxia at distances beyond the diffusion capacity of oxygen (typically about 200 μm) [17]. Beyond this distance, the innermost cells of the spheroid may have difficulty accessing the supply of oxygen and fresh growth medium to thrive. To prevent necrosis of the spheroid core, we opted for spheroids formed with a seeding density of 2.50×10^4 cells/ cm^2 in the following experiments. The ASC aggregates grown at this cell seeding density had an average diameter of approximately 150 μm after 7 days of culture.

Under electron microscope, cells on the surface of the spheroid appeared to aggregate together tightly (Fig. 2b), and it was difficult to distinguish the cellular boundary. The viability of these cell

spheroids was assessed using a live/dead assay. Cells that lost membrane integrity and were no longer viable were stained red, while the viable cells were stained green. As shown in Fig. 2c, the majority of the cells in aggregates was viable, based on the fluorescence images of 50 optical sections. We also performed trypan blue dye exclusion assay to assess the percentage of viable ASCs in monolayer and spheroid-derived cells. On day 1, 3, 5, and 7, the percentages of viable cells of monolayer and spheroid origin were high (>95%) and exhibited no statistical significant difference among different groups (Fig. 2d).

3.2. Phenotypic characterization of spheroid ASCs

We analyzed the expression of a panel of cell surface antigens in parallel monolayer and spheroid ASCs after 7 days of culture. We confirmed that mesenchymal stem cell-related markers, including CD90 and CD105, were expressed by a high percentage of monolayer ASCs and lacked expression of the hematopoietic markers

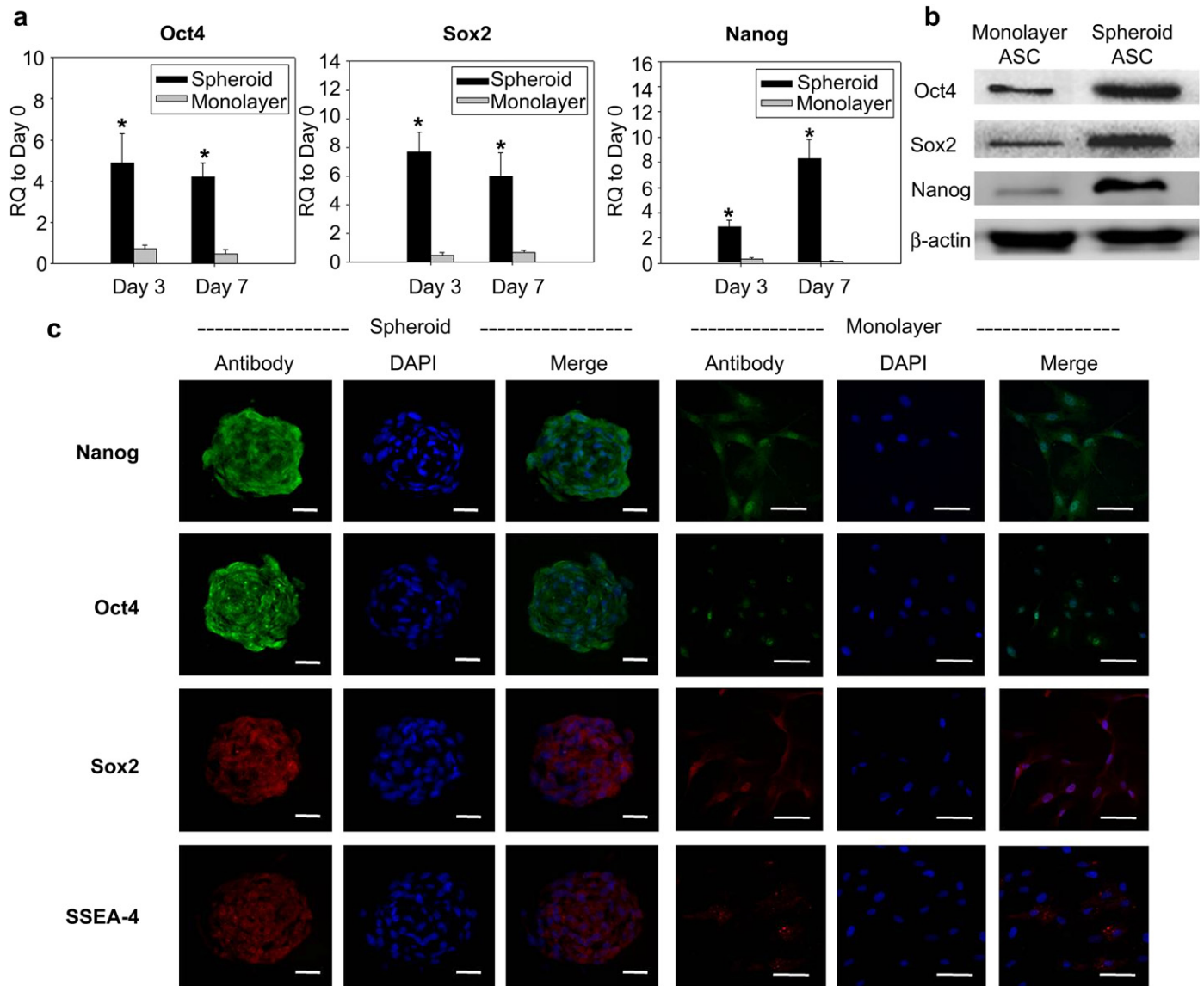


Fig. 5. (a) RT-PCR measurements for embryonic stem cell marker genes (*Oct-4*, *Sox-2* and *Nanog*) in monolayer and spheroid ASCs. Values are mean RQ \pm SD compared with day 0 ASC sample; * $p < 0.05$, compared to the monolayer group ($n = 3$). (b) Western blot analysis of the expression of embryonic stem cell markers *Oct-4*, *Sox-2* and *Nanog* in monolayer and spheroid ASCs. (c) Representative immunostaining of *Oct-4*, *Sox-2*, *Nanog* and SSEA-4 in ASC spheroid and monolayer after 7 days of culture. All nuclei were stained with DAPI (blue). Scale bar: 50 μm . (For interpretation of the references to colour in this figure legend, the reader is referred to the web version of this article.)

CD34 and PECAM. The surface epitopes of spheroid ASCs were different from the surface epitopes of ASCs from adherent monolayers when dissociated under the same conditions with trypsin (10 min at 37 °C). ASCs in the spheroid showed a decrease in the expression levels of markers CD29, CD90, and CD105, along with an increase in the expression of CD34, CD44, and PECAM (Fig. 3a).

We further examined the ratio of apoptotic and necrotic cells of monolayer and spheroid culture under serum-free condition. For ASC spheroids, $98.7 \pm 0.1\%$ of the harvested cells were viable as assayed by PI uptake and labeling with annexin V-FITC, which was significantly higher than the ratio of $84.8 \pm 2.0\%$ in the monolayer group (Fig. 3b). Moreover, immunohistochemistry revealed a robust meshwork of fibronectin and laminin inherent with its endogenous ECM in ASC spheroids. In contrast, fibronectin and laminin immunostaining of monolayer ASC culture was far less obvious (Fig. 4a). RT-PCR analysis also revealed 3.6 ± 0.8 fold upregulated *Fibronectin* and 51.4 ± 5.4 fold upregulated *Laminin- α 1* genes in ASC spheroids comparing to D0 ASCs, and both exhibited significantly more transcripts than monolayer culture (Fig. 4b).

3.3. The expression of pluripotent marker genes in ASC spheroid

The relative mRNA expression of pluripotency-associated transcription factors *Sox-2*, *Oct-4* and *Nanog* was analyzed by qPCR. In comparison to monolayer cells, the ASC spheroids exhibited

significant upregulation of *Sox-2*, *Oct-4* and *Nanog* genes on day 3, with 7.7-fold, 4.9-fold and 2.9-fold increase from day 0 ASCs respectively. On day 7, the transcript numbers of *Sox-2*, *Oct-4* and *Nanog* genes were still higher in the spheroid group, with 6.0-fold, 4.2-fold and 8.3-fold increase from day 0 ASCs respectively (Fig. 5a). Western blot analysis also showed more protein expression of *Sox-2*, *Oct-4* and *Nanog* in ASC spheroids comparing to monolayer culture (Fig. 5b). Analyses of immunofluorescence images further confirmed the expression of these stemness markers, as well as another important pluripotency marker, SSEA-4, in ASC spheroids (Fig. 5c).

3.4. Regenerative capability of spheroid ASCs

Upon seeding ASC spheroids back to TCPS, the cells in spheroids demonstrated adherence to TCPS and gradually spread out from day 1 to day 7. Furthermore, there was a 2.5-fold increase in the activity index on day 3 after seeding ASC spheroids back to TCPS, followed by a 3.2-fold increase on day 5 and a 2.7-fold increase on day 7. In contrast, the activity indices did not change significantly when the spheroids were seeded back to a new chitosan film (Fig. 6a).

To evaluate the proliferation potential of cells within the spheroids, ASC spheroids were dissociated with trypsin and seeded back to TCPS. Comparing to monolayer ASCs, spheroid-derived

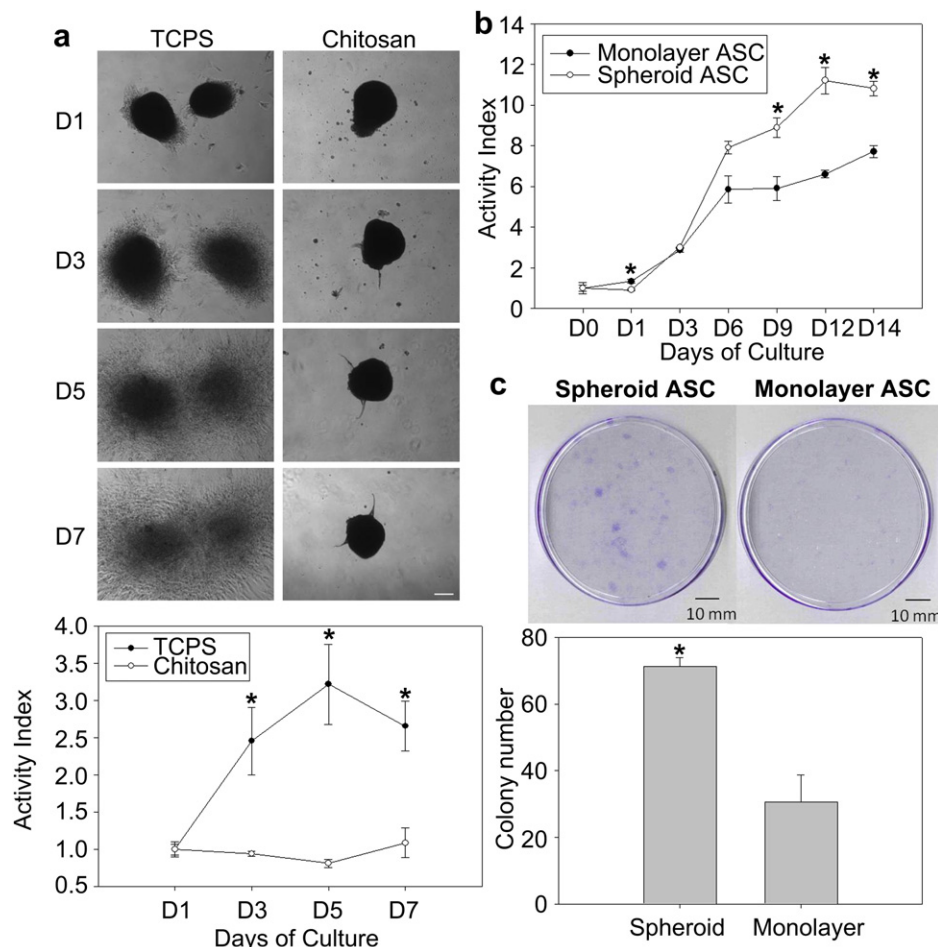


Fig. 6. (a) Upon transferring to TCPS, ASC spheroids attached to the TCPS surface and cells started to migrate from the spheroids to proliferate on TCPS, while the ASC spheroids remained intact when transferred to a new chitosan surface. Scale bar: 150 μ m. Alamar blue assay for ASC spheroids transferred to TCPS showed significantly more cellular proliferation than those seeded on new chitosan films. Day 0 was defined as the day of seeding spheroids. (b) Alamar blue assays of monolayer ASCs (solid circle) and spheroid-derived ASCs (empty circle) on TCPS at the seeding density of 2.50×10^4 cells/cm². (c) CFU-F assays of ASCs plated at 1000 cells/dish and incubated for 14 days. Values are mean colony number \pm SD; * $p < 0.05$, compared to the monolayer group ($n = 3$).

ASCs exhibited a slower growth in the beginning, but their activity index became significantly higher at the later time points (Fig. 6b). In addition, the dissociated cells readily generated colony-forming units (CFUs) when plated at clonal densities. After 14 days of culture, the number of CFUs from spheroid cells was significantly more than the number of CFUs from adherent cultures (71.3 ± 2.5 vs. 30.6 ± 8.1 , Fig. 6c).

3.5. Differentiation capabilities of ASC spheroids

ASC spheroids on chitosan films maintained the capabilities of adipogenic and osteogenic differentiation after appropriate induction media were applied, as demonstrated by the histology staining specific for oil and calcium, respectively (Fig. 7a). Determination of relative gene expression levels by qPCR showed no significantly different transcript levels of *PPAR- γ* after between adipogenically induced ASC spheroids and monolayer ASCs. However, *Runx2* gene was significantly upregulated in spheroids comparing to monolayer ASCs after osteogenic induction (Fig. 7b).

While spheroid formation maintained the differentiation capabilities along the mesenchymal lineages of ASC, we also observed enhanced transdifferentiation capabilities of ASC spheroids. RT-PCR revealed significantly more gene transcripts of *Nestin* and *Albumin* in spheroids comparing to monolayer ASCs after appropriate neurogenic or hepatogenic induction media was applied respectively. Immunofluorescence analyses of these two important neurogenic and hepatogenic differentiation markers further confirmed the protein expression of *Nestin* and *Albumin* in ASC spheroids (Fig. 8a and b).

3.6. Engraftment of monolayer and spheroid ASCs in vivo

ASC spheroids and dissociated monolayer ASCs with comparable cell numbers were transplanted into hindlimbs of nude mice by intramuscular injection. Tissue samples were retrieved at day 7 and 21 postoperatively, and immunohistochemistry for HNA was performed to identify the transplanted cells (Fig. 9a). On both time points, significantly more HNA-positive cells were observed per high power field in the spheroid injection group. Comparing to the mice that received dissociated ASCs, HNA-positive cells per field was 4 times more in the mice that received spheroid injection (106 ± 18 vs. 27 ± 13) on day 7, and the ratio increased to 13 (92 ± 29 vs. 7 ± 7) on day 21 (Fig. 9b).

4. Discussion

Stem cells have the ability to renew themselves, so they are considered as good cell sources for tissue engineering. When appropriate microenvironment and stimuli are applied, stem cells can differentiate into specialized cell types. ESCs can differentiate into virtually every kind of specialized cell in human bodies. However, the use of fertilized eggs to harvest ESCs is ethically controversial [32], which has rendered the clinical application of ESCs more difficult. On the contrary, tissue-specific adult stem cells, particularly MSCs, exhibit few ethical issues regarding their procurement, and thus have drawn much attention to their potential application in tissue regeneration [1,33–35]. These cells have been known for years for their capacity to differentiate along their lineage of origin. However, several recent reports have shown that

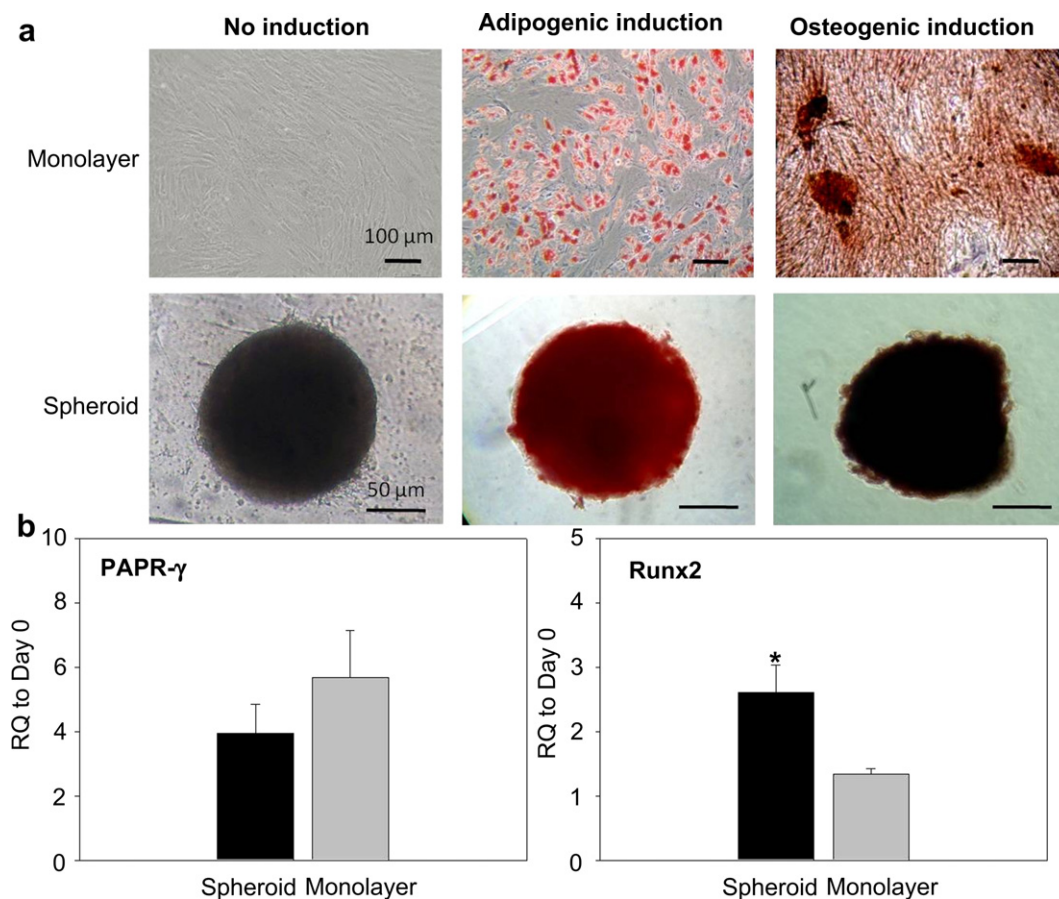


Fig. 7. (a) Microscopic images of monolayer and spheroid ASCs cultured in adipogenic, osteogenic and non-induction medium for 14 days. Cell cultures were stained with Oil Red O for detection of adipogenesis and Alizarin Red for detection of osteogenesis. Scale bars: monolayer, 100 μ m; spheroid, 50 μ m. (b) RT-PCR measurements for adipogenic and osteogenic marker genes (*PPAR- γ* and *Runx2*, respectively) in monolayer and spheroid ASCs. Values are mean RQ \pm SD; * $p < 0.05$, compared to the monolayer group ($n = 3$).

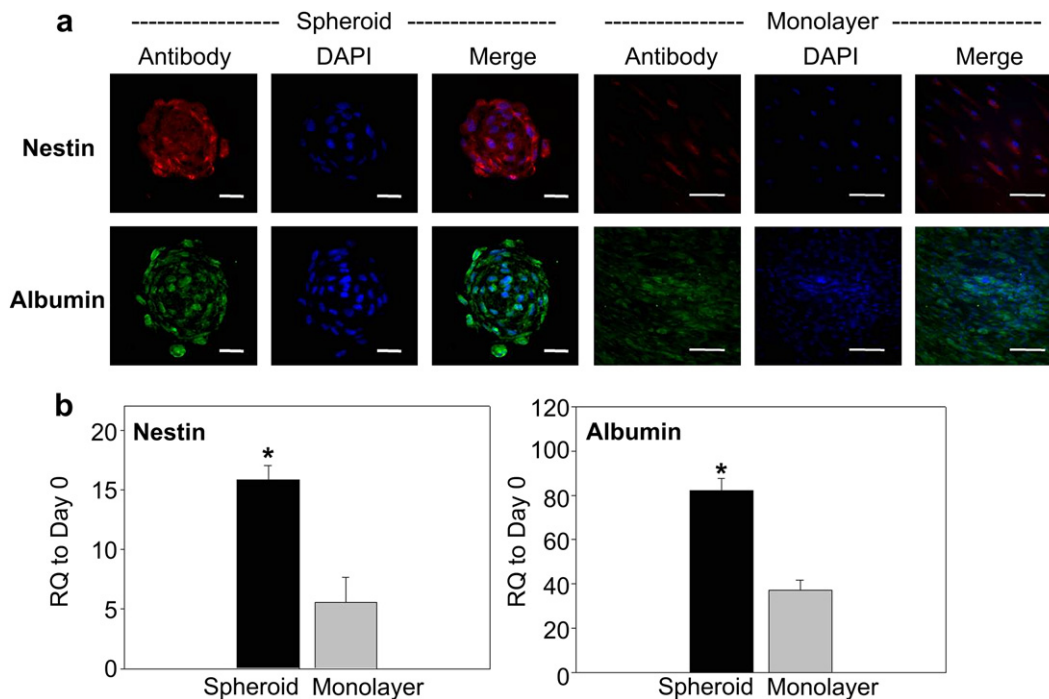


Fig. 8. (a) Immunofluorescence images of monolayer and spheroid ASCs cultured in neurogenic and hepatogenic medium for 14 days. Cell cultures were stained with Nestin for neurogenic induction and albumin for hepatogenic induction. Scale bar: 50 μm . (b) RT-PCR measurements for neurogenic and hepatogenic marker genes (*Nestin* and *Albumin*, respectively) in monolayer and spheroid ASCs. Values are mean RQ \pm SD; * $p < 0.05$, compared to the monolayer group ($n = 3$).

adult stem cell populations, isolated from various tissues in the mature organism, are capable of differentiating into mature cells not related with their original lineage [36,37]. This wide range of plasticity was previously considered to be an exclusive characteristic of ESCs. The maintenance of pluripotency in ESCs has been attributed to several important transcription factors, including *Oct-4*, *Sox-2* and *Nanog* [38]. The presence of these pluripotency markers has also been identified in adult stem cells, including ASCs, and they exert great influence on the renewal and differentiation capabilities [7,8]. However, the expression of several pluripotent genes declined with *in vitro* passaging of ASCs [9], and it is thus important to develop techniques to preserve stemness [8]. The experiments presented here were designed to prepare ASCs as spheroids on chitosan films, thereby enhancing their stem cell characteristics, including capabilities for expansion and differentiation.

The advance in molecular technologies has enabled the manipulation of transcriptional code and epigenetic state to induce pluripotency in mature adult cells, resulting in induced pluripotent (iPS) cells [39,40]. Human ASCs can be reprogrammed to iPS cells with substantially higher efficiencies than those reported for human fibroblasts in feeder-free conditions [41], which suggested that ASCs remain in a relatively immature state that is prone to reprogramming to ground state pluripotency. Certainly, introducing transcription factors to multipotent MSCs can lead to reprogramming and alter the cell fate, thereby making transdifferentiation possible [36]. Nevertheless, genetically modified cells elicit great safety concern and are very difficult to apply in clinical settings. In the present study, we demonstrated that ASCs on chitosan films were able to form 3D spheroids shortly after cell seeding on chitosan films, and the expression of stemness markers (*Oct-4*, *Sox-2* and *Nanog*) was upregulated in these spheroids. The spheroid ASCs also displayed a quite different pattern of cell surface markers comparing to monolayer cells. The decrease of mesenchymal markers (CD90 and CD105) also suggested that ASCs within spheroids were shifting away from mesenchymal lineage, probably de-differentiating to

a more primitive state. In previous studies, bone marrow-derived MSC spheroids showed more efficient osteogenic or adipogenic differentiation [21,42]. We further demonstrated that ASC spheroids exhibited significantly enhanced neurogenic (ectoderm) and hepatogenic (endoderm) transdifferentiation capabilities comparing to monolayer controls, demonstrated by upregulated *Nestin* and *Albumin* genes when cultured in appropriate induction media. In the mean time, adipogenic and osteogenic (mesoderm) differentiation capacities of ASCs were still maintained after spheroid formation.

Growing stem cells as spheres has been described in many research fields, such as tumorigenesis, pharmacogenetics, embryoid body formation from ESCs, and neurospheres from neuroprogenitors [43]. Bone marrow-derived MSCs have been induced to form 3D spheroids in recent years by culturing cells in hanging drops [20], in microwells [17] or on micropatterned surfaces [21,42]. Because MSCs within spheroids have less access to oxygen and nutrients, it was of interest to know whether more cells within the spheroid undergo apoptosis. In fact, most of the cells within aggregates were shown to be viable in these studies, which corresponded to our results [17,20,21]. Moreover, we showed that ASCs within the spheroid are more resistant to a hazardous serum-free culture condition, and they resumed an even higher expansion and colony-forming capabilities after transferring from chitosan surface to TCPS. Comparing to monolayer ASCs, we also demonstrated significantly higher fibronectin and laminin expressions in ASC spheroids. For most types of cells, the opportunities for attachment and proliferation depend on their surrounding ECM, which are inherent with the seeded cell aggregate. For example, bone marrow-derived MSC aggregates in microwells preserved their endogenous ECM and thus facilitated cell transplantation [17]. In this study, a higher cellular retention rate was also observed after intramuscular injection of ASC spheroids in a nude mice model.

The molecular forces that increase expression of pluripotent marker genes in ASC spheroids are intriguing but unclear. ASCs in spheroids are more rounded comparing to the flat cells on TCPS, and

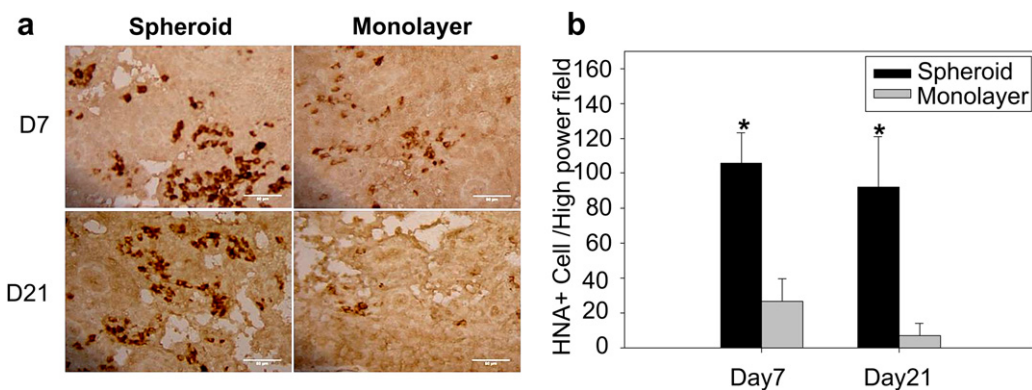


Fig. 9. (a) Immunohistochemical images of human nuclear antigen (HNA). Muscle samples were obtained from the groups treated with ASC spheroids or dissociated monolayer ASCs at postoperative day 7 and 21. HNA-immunostained cells represent the transplanted ASCs. Scale bar: 50 μ m. (b) Number of HNA-positive cell calculated from 10 randomly selected high power fields per sample. Values are mean cell number per high power field \pm SD; * $p < 0.05$, compared to the monolayer group ($n = 4$).

cell shape alone has been demonstrated to regulate the gene expression and protein production of cells for specific applications [44]. Moreover, cells in spheroids are in close association with each other and probably can provide signal cues to each other much easier than in monolayer cultures, where a cell can only touch very limited neighboring cells in a 2D manner, and secreted molecules must be present in high amounts to ensure effective communication [20]. The changes in ASCs as they form spheroids are probably the result of the nonadherent culture conditions, high degree of confluency, and nutrient/oxygen deprivation. For example, hypoxic culture condition has been shown to enhance the stemness of several kinds of stem cells [45–47]. However, serum-free culture of human ASCs in commercially available low attachment flasks showed no significant upregulation of *Oct-4* and *Nanog* gene expression after spheroid formation [48]. Hence, forming spheroid alone may not account for the observation of enhanced ASC stemness in this study. Dynamic interaction among the ASC spheroids on chitosan membranes, as demonstrated by the time-lapse microscopic image, and the medium in which the spheroids are cultured probably also play important roles. More detailed studies of each of these and other possible factors should be conducted to have a better understanding of the changes of ASC phenotypes when they aggregate into spheroids.

5. Conclusions

The results presented here indicated that ASCs can be activated nonchemically on chitosan films to form spheroids and express pluripotent marker genes. During *in vitro* culture, most ASCs in the spheroid remained viable, produce more ECM molecules, and were more resistant to a hazardous serum-free environment. Moreover, ASCs dissociated from spheroids displayed higher expansion activity and colony-forming activity. When cultured in appropriate media, ASC spheroids demonstrated enhanced transdifferentiation capabilities into neuron and hepatocyte. In a nude mice model, human ASC spheroids exhibited better cellular retention after intramuscular injection in comparison to the dissociated monolayer cells. Therefore, spheroid ASCs formed on chitosan films may have potential advantages for many clinical applications.

Acknowledgments

The project was supported by the National Science Council of Taiwan, National Taiwan University Hospital, and E-Da Hospital – National Taiwan University Hospital Joint Research Program. The authors also acknowledge the technical assistance from the staff of the Eighth Core Lab of National Taiwan University Hospital.

Appendix. Supplementary information

Supplementary video related to this article can be found at doi: [10.1016/j.biomaterials.2011.11.049](https://doi.org/10.1016/j.biomaterials.2011.11.049).

References

- Gimble JM, Guilak F. Differentiation potential of adipose derived adult stem (ADAS) cells. *Curr Top Dev Biol* 2003;58:137–60.
- Aust L, Devlin B, Foster SJ, Halvorsen YD, Hicok K, du Laney T, et al. Yield of human adipose-derived adult stem cells from liposuction aspirates. *Cytotherapy* 2004;6:7–14.
- Fraser JK, Wulur I, Alfonso Z, Hedrick MH. Fat tissue: an underappreciated source of stem cells for biotechnology. *Trends Biotechnol* 2006;24:150–4.
- Guilak F, Lott KE, Awad HA, Cao Q, Hicok KC, Fermor B, et al. Clonal analysis of the differentiation potential of human adipose-derived adult stem cells. *J Cell Physiol* 2006;206:229–37.
- Anghileri E, Marconi S, Pignatelli A, Cifelli P, Galie M, Sbarbati A, et al. Neuronal differentiation potential of human adipose-derived mesenchymal stem cells. *Stem Cells Dev* 2008;17:909–16.
- Banas A, Teratani T, Yamamoto Y, Tokuhara M, Takeshita F, Quinn G, et al. Adipose tissue-derived mesenchymal stem cells as a source of human hepatocytes. *Hepatology* 2007;46:219–28.
- Riekstina U, Cakstina I, Parfejevs V, Hoogduijn M, Jankovskis G, Muiznieks I, et al. Embryonic stem cell marker expression pattern in human mesenchymal stem cells derived from bone marrow, adipose tissue, heart and dermis. *Stem Cell Rev* 2009;5:378–86.
- Baer PC, Griesche N, Luttmann W, Schubert R, Luttmann A, Geiger H. Human adipose-derived mesenchymal stem cells in vitro: evaluation of an optimal expansion medium preserving stemness. *Cytotherapy* 2010;12:96–106.
- Park E, Patel AN. Changes in the expression pattern of mesenchymal and pluripotent markers in human adipose-derived stem cells. *Cell Biol Int* 2010;34:979–84.
- Watt FM, Hogan BL. Out of Eden: stem cells and their niches. *Science* 2000;287:1427–30.
- Bartosh TJ, Wang Z, Rosales AA, Dimitrijevič SD, Roque RS. 3D-model of adult cardiac stem cells promotes cardiac differentiation and resistance to oxidative stress. *J Cell Biochem* 2008;105:612–23.
- Frith JE, Thomson B, Genever PG. Dynamic three-dimensional culture methods enhance mesenchymal stem cell properties and increase therapeutic potential. *Tissue Eng C Methods* 2010;16:735–49.
- Lin SJ, Jee SH, Hsiao WC, Yu HS, Tsai TF, Chen JS, et al. Enhanced cell survival of melanocyte spheroids in serum starvation condition. *Biomaterials* 2006;27:1462–9.
- Young TH, Lee CY, Chiu HC, Hsu CJ, Lin SJ. Self-assembly of dermal papilla cells into inductive spheroidal microtissues on poly(ethylene-co-vinyl alcohol) membranes for hair follicle regeneration. *Biomaterials* 2008;29:3521–30.
- Cheng NC, Estes BT, Awad HA, Guilak F. Chondrogenic differentiation of adipose-derived adult stem cells by a porous scaffold derived from native articular cartilage extracellular matrix. *Tissue Eng A* 2009;15:231–41.
- Chen MH, Chen YJ, Liao CC, Chan YH, Lin CY, Chen RS, et al. Formation of salivary acinar cell spheroids in vitro above a polyvinyl alcohol-coated surface. *J Biomed Mater Res A* 2009;90:1066–72.
- Lee WY, Chang YH, Yeh YC, Chen CH, Lin KM, Huang CC, et al. The use of injectable spherically symmetric cell aggregates self-assembled in a thermo-responsive hydrogel for enhanced cell transplantation. *Biomaterials* 2009;30:5505–13.
- Sekine H, Shimizu T, Hobo K, Sekiya S, Yang J, Yamato M, et al. Endothelial cell coculture within tissue-engineered cardiomyocyte sheets enhances neovascularization and improves cardiac function of ischemic hearts. *Circulation* 2008;118:S145–52.

- [19] Yeh YC, Lee WY, Yu CL, Hwang SM, Chung MF, Hsu LW, et al. Cardiac repair with injectable cell sheet fragments of human amniotic fluid stem cells in an immune-suppressed rat model. *Biomaterials* 2010;31:6444–53.
- [20] Bartosh TJ, Ylostalo JH, Mohammadipoor A, Bazhanov N, Coble K, Claypool K, et al. Aggregation of human mesenchymal stromal cells (MSCs) into 3D spheroids enhances their antiinflammatory properties. *Proc Natl Acad Sci U S A* 2010;107:13724–9.
- [21] Wang W, Itaka K, Ohba S, Nishiyama N, Chung UI, Yamasaki Y, et al. 3D spheroid culture system on micropatterned substrates for improved differentiation efficiency of multipotent mesenchymal stem cells. *Biomaterials* 2009;30:2705–15.
- [22] Shi C, Zhu Y, Ran X, Wang M, Su Y, Cheng T. Therapeutic potential of chitosan and its derivatives in regenerative medicine. *J Surg Res* 2006;133:185–92.
- [23] Lin SJ, Jee SH, Hsiao WC, Lee SJ, Young TH. Formation of melanocyte spheroids on the chitosan-coated surface. *Biomaterials* 2005;26:1413–22.
- [24] Yang TL, Young TH. The specificity of chitosan in promoting branching morphogenesis of progenitor salivary tissue. *Biochem Biophys Res Commun* 2009;381:466–70.
- [25] Yeh LK, Chen YH, Chiu CS, Hu FR, Young TH, Wang JJ. The phenotype of bovine corneal epithelial cells on chitosan membrane. *J Biomed Mater Res A* 2009;90:18–26.
- [26] Chatelet C, Damour O, Domard A. Influence of the degree of acetylation on some biological properties of chitosan films. *Biomaterials* 2001;22:261–8.
- [27] Chen YH, Wang JJ, Young TH. Formation of keratocyte spheroids on chitosan-coated surface can maintain keratocyte phenotypes. *Tissue Eng A* 2009;15:2001–13.
- [28] Ahmed SA, Gogal Jr RM, Walsh JE. A new rapid and simple non-radioactive assay to monitor and determine the proliferation of lymphocytes: an alternative to [³H]thymidine incorporation assay. *J Immunol Methods* 1994;170:211–24.
- [29] Battula VL, Bareiss PM, Tremel S, Conrad S, Albert I, Hojak S, et al. Human placenta and bone marrow derived MSC cultured in serum-free, b-FGF-containing medium express cell surface frizzled-9 and SSEA-4 and give rise to multilineage differentiation. *Differentiation* 2007;75:279–91.
- [30] Jang S, Cho HH, Cho YB, Park JS, Jeong HS. Functional neural differentiation of human adipose tissue-derived stem cells using bFGF and forskolin. *BMC Cell Biol* 2010;11:25.
- [31] Coradeghini R, Guida C, Scanarotti C, Sanguineti R, Bassi AM, Parodi A, et al. A comparative study of proliferation and hepatic differentiation of human adipose-derived stem cells. *Cells Tissues Organs* 2010;191:466–77.
- [32] Cohen IG, Adashi EY. Human embryonic stem-cell research under siege – battle won but not the war. *N Engl J Med* 2011;364:e48.
- [33] Vormoor J, Lapidot T, Pflumio F, Risdon G, Patterson B, Broxmeyer HE, et al. Immature human cord blood progenitors engraft and proliferate to high levels in severe combined immunodeficient mice. *Blood* 1994;83:2489–97.
- [34] Lemischka IR, Raulet DH, Mulligan RC. Developmental potential and dynamic behavior of hematopoietic stem cells. *Cell* 1986;45:917–27.
- [35] Lavker RM, Sun TT. Epidermal stem cells: properties, markers, and location. *Proc Natl Acad Sci U S A* 2000;97:13473–5.
- [36] Barzilay R, Melamed E, Offen D. Introducing transcription factors to multipotent mesenchymal stem cells: making transdifferentiation possible. *Stem Cells* 2009;27:2509–15.
- [37] Barzilay R, Kan I, Ben-Zur T, Bulvik S, Melamed E, Offen D. Induction of human mesenchymal stem cells into dopamine-producing cells with different differentiation protocols. *Stem Cells Dev* 2008;17:547–54.
- [38] Loh KM, Lim B. A precarious balance: pluripotency factors as lineage specifiers. *Cell Stem Cell* 2011;8:363–9.
- [39] Silva J, Barrandon O, Nichols J, Kawaguchi J, Theunissen TW, Smith A. Promotion of reprogramming to ground state pluripotency by signal inhibition. *PLoS Biol* 2008;6:e253.
- [40] Takahashi K, Tanabe K, Ohnuki M, Narita M, Ichisaka T, Tomoda K, et al. Induction of pluripotent stem cells from adult human fibroblasts by defined factors. *Cell* 2007;131:861–72.
- [41] Sugii S, Kida Y, Kawamura T, Suzuki J, Vassena R, Yin YQ, et al. Human and mouse adipose-derived cells support feeder-independent induction of pluripotent stem cells. *Proc Natl Acad Sci U S A* 2010;107:3558–63.
- [42] Miyagawa Y, Okita H, Hiroshima M, Sakamoto R, Kobayashi M, Nakajima H, et al. A microfabricated scaffold induces the spheroid formation of human bone marrow-derived mesenchymal progenitor cells and promotes efficient adipogenic differentiation. *Tissue Eng A* 2011;17:513–21.
- [43] Wartenberg M, Gunther J, Hescheler J, Sauer H. The embryoid body as a novel in vitro assay system for antiangiogenic agents. *Lab Invest* 1998;78:1301–14.
- [44] Shao HJ, Lee YT, Chen CS, Wang JH, Young TH. Modulation of gene expression and collagen production of anterior cruciate ligament cells through cell shape changes on polycaprolactone/chitosan blends. *Biomaterials* 2010;31:4695–705.
- [45] Bhang SH, Cho SW, La WG, Lee TJ, Yang HS, Sun AY, et al. Angiogenesis in ischemic tissue produced by spheroid grafting of human adipose-derived stromal cells. *Biomaterials* 2011;32:2734–47.
- [46] Forristal CE, Wright KL, Hanley NA, Oreffo RO, Houghton FD. Hypoxia inducible factors regulate pluripotency and proliferation in human embryonic stem cells cultured at reduced oxygen tensions. *Reproduction* 2010;139:85–97.
- [47] Tsai CC, Chen YJ, Yew TL, Chen LL, Wang JY, Chiu CH, et al. Hypoxia inhibits senescence and maintains mesenchymal stem cell properties through down-regulation of E2A-p21 by HIF-TWIST. *Blood* 2011;117:459–69.
- [48] Dromard C, Bourin P, Andre M, De Barros S, Casteilla L, Planat-Benard V. Human adipose derived stroma/stem cells grow in serum-free medium as floating spheres. *Exp Cell Res* 2011;317:770–80.